Plant virus evolution under strong drought conditions results in a transition from parasitism to mutualism

Rubén González[1], Anamarija Butković[1], Francisco J. Escaray[2], Javier Martínez-Latorre[1], Ízan Melero[1], Enric Pérez-Parets[1], Aurelio Gómez-Cadenas[3], Pedro Carrasco[2], and Santiago F. Elena[1,4,*]

[1]Instituto de Biología Integrativa de Sistemas (I[2]SysBio), CSIC-Universitat de València, Paterna, 46980 Valencia, Spain.

[2]Departament de Bioquímica i Biologia Molecular and ERI Biotecnologia i Biomedicina (BIOTECMED), Universitat de València, Burjassot, 46100 Valencia, Spain.

[3]Departament de Ciències Agràries i del Medi Natural, Universitat Jaume I, Castelló de la Plana, 12071 Castellón, Spain.

[4]Santa Fe Institute, Santa Fe NM 87501, USA

[*]Corresponding author E-mail: santiago.elena@csic.es

Keywords: *Arabidopsis thaliana*, drought tolerance, experimental evolution, gene expression, hormone signaling, mutualism, *Potyvirus*, Systems Biology, virus evolution

Environmental conditions are an important factor driving pathogens evolution. Here we explore the effects of drought stress in plant virus evolution. We evolved a potyvirus in well-watered and drought conditions in *Arabidopsis thaliana* accessions that differ in their response to virus infection. Virus adaptation occurred in all accessions independently of watering status. Drought-evolved viruses conferred a significantly higher tolerance to drought to infected plants. By contrast, non-significant increases in tolerance were observed in plants infected with viruses evolved under standard watering. The magnitude of this effect was dependent on the plant accessions. Differences in tolerance were correlated to alterations in the expression of host genes, some involved in regulation of the circadian clock, as well as in deep changes in the balance of phytohormones regulating defense and growth signaling pathways. Our results show that viruses can promote host survival in situations of abiotic stress, being the magnitude of such benefit a selectable trait.

Viruses are the most abundant biological entities, having an enormous diversity and a ubiquitous distribution[1]. Traditionally, they have been studied in the context of disease but nowadays numerous beneficial viruses are being identified in a diverse range of host species[2]. Wild plant populations are frequently asymptomatically infected with viruses that in some cases produce diseases in cultivated plants[3]. This happens because host-virus interactions fall on a spectrum between pathogenesis and mutualism and during their lifecycle viruses might switch between these two lifestyles[4,5]. This evolutionary transition may happen depending on the environment and the genetics of hosts and viruses[6,7]. In summary, interactions between plant viruses and their wild hosts often do not result in apparent costs for the host.

Plants, as the sessile organisms they are, must also deal with frequent environmental abiotic perturbations. To face these abiotic stresses, plants have evolved mechanisms to acclimate and tolerate perturbations. Plant responses triggered by some stressors interacts with the response caused by others, such is the case for drought and cold[8]. This also happens between abiotic and biotic stressors[9,10], meaning that under certain environmental circumstances (*i.e.*, perturbations in water availability, extreme temperatures, excess of light irradiation, or oxidative stress) even pathogenic viruses can be beneficial for their host, since virus infection can induce changes in the host physiological homeostasis that may help it to survive under these adverse circumstances[7]. Drought is one of the main stressors for plants that, depending on its intensity and duration, causes major fitness reductions or even the organism's death. This stress is predicted to have a severe and widespread effect by the second half of the XXIst century as a result of the expected decrease in precipitation and/or increase in evaporation due to higher temperatures[11]. Xu et al. showed that plants infected with certain viruses can improve their tolerance to

drought[12]. It has been shown that the combination of drought and infection with turnip mosaic virus (TuMV; genus *Potyvirus*, family *Potyviridae*) affects different signaling networks in *Arabidopsis thaliana* (L.) Heynh plants[13]. Similarly, *Nicotiana benthamiana* Domin plants infected with fungal endophytes and yellow tailflower mild mottle virus become more tolerant to drought stress due to the modulation of osmolytes, antioxidant enzymes and drought responsive genes[14]. (Additional examples have been recently summarized in ref. 7). Environmental perturbations can also affect pathogens evolution as changes in the environment can influence the specificity of selection[15].

Here we study how severe drought influences virus evolution. Using experimental evolution, we have characterized changes occurring in the virus genome and in the host-virus interactions, paying special attention to changes in the host's transcriptome and hormonal profiles. We have evolved TuMV in four different natural accessions of *A. thaliana* that vary in their responses to infection with potyviruses[16,17]. These accessions classified into two groups according to their phenotypic and transcriptomic responses[17]: accessions in Group 1 (G1) L*er*-0 and St-0 showed severe symptoms and strong induction of defense genes, while Oy-0 and Wt-1 in Group 2 (G2) showed milder symptoms and over expression of genes involved in abiotic stress. An *A. thaliana*-naïve TuMV isolate, hereafter referred as the ancestral, was evolved in each of the accessions during five experimental passages in standard watering or drought conditions.

Results and Discussion

TuMV evolution under standard and drought conditions. At the end of the evolution experiment (Fig. 1A) we obtained 12 lineages evolved in standard and 10

87 in drought conditions (two of the lineages evolved in Wt-1 under drought conditions
88 became extinct before reaching passage five). All resulting viral lineages had
89 experienced significant increases in their area under the disease progress stairs
90 (*AUDPS*)[18], a value that summarizes both infectivity and the speed of inducing
91 symptoms (Fig. 1B). For the viral lineages evolved in G1 accessions, the increase in
92 *AUDPS* was significantly higher when plants were grown in standard (mean
93 difference with ancestral ±1 SD: 3.450 ±0.411 in L*er*-0 and 1.900 ±0.262 in St-0;
94 Fig. 1B) than in drought conditions (2.733 ±0.395 in L*er*-0 and 1.200 ±0.310 in St-
95 0; Fig. 1B). Viruses evolved in G2 accessions also showed a significant increase in
96 *AUDPS* relative to the ancestral virus, but this increase was larger for the lineages
97 evolved in plants grown in drought conditions (2.467 ±0.304 in Oy-0 and in 4.841
98 ±0.301 in Wt-1; Fig. 1B) compared to the standard conditions (1.771 ±0.229 in Oy-
99 0 and 4.309 ±0.176 in Wt-1; Fig. 1B). When facing abiotic stress, plants adjust their
100 metabolism and gene expression to adapt to the stress[19]. These physiological changes
101 induced by the environment may have an effect in the outcome of a virus infection,
102 facilitating or jeopardizing virus adaptation depending on the host genetics.
103 Next, seeking to characterize the spectrum of mutations that appeared in the
104 evolved viral genomes, the nucleotide sequences of the ancestral and evolved viruses
105 were obtained (Fig. 1C). Viruses evolved in standard conditions accumulated 32
106 mutations, five were fixed and 27 were polymorphisms. Nonsynonymous
107 substitutions were the most common type, 27 out of 32 mutations. These mutations
108 were not randomly distributed along the viral genome, but mainly concentrated in the
109 *VPg* cistron (15 out of 32). Viruses evolved in drought conditions accumulated 26
110 mutations, only one was fixed and 25 remained polymorphisms. Again, most
111 mutations were nonsynonymous (21) and preferentially were observed in the *VPg*

112 cistron. Interestingly, all mutations observed in the *VPg* fall within a narrow domain
113 encompassing amino acids 107 - 120 of the protein (Supplementary Fig. S1).
114

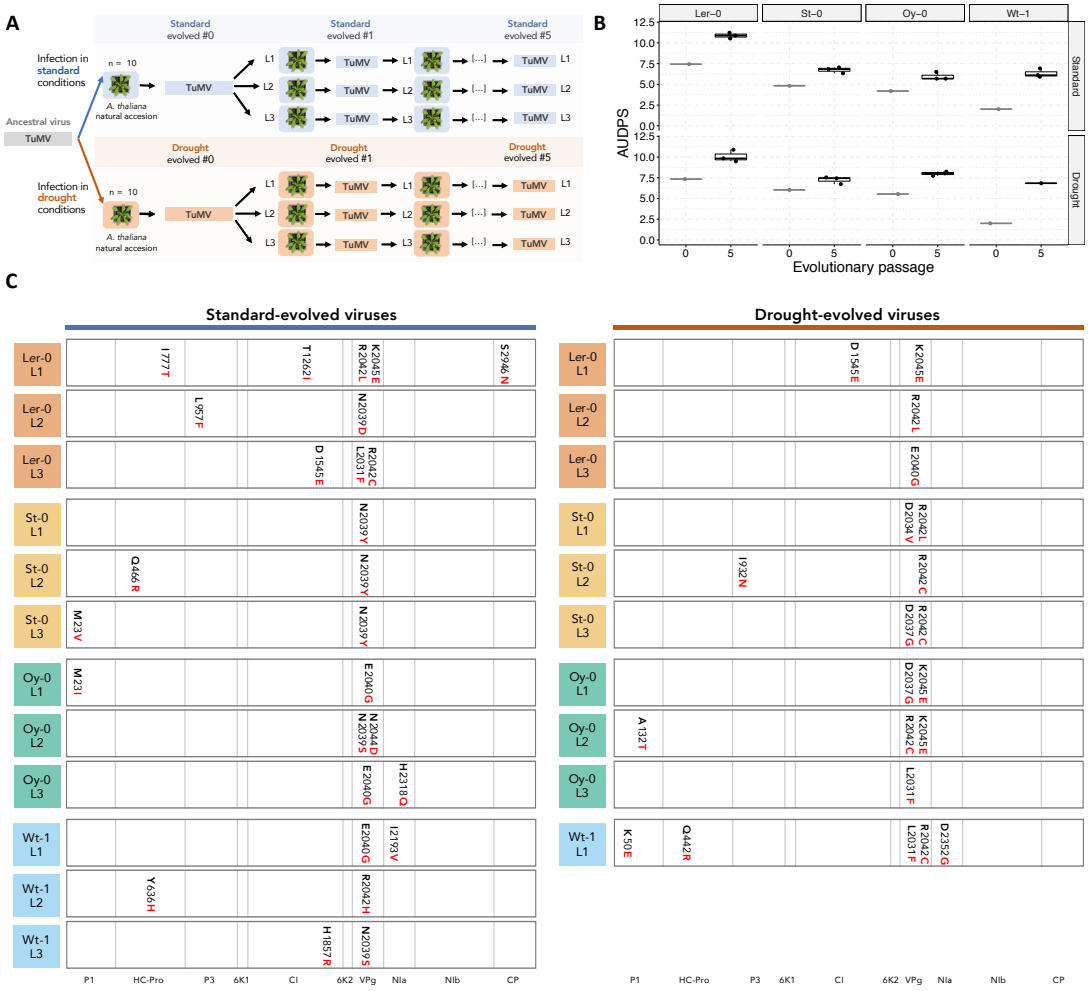

Fig. 1. Experimental evolution of TuMV lineages. (A) Experimental design of the evolution experiment. (B) *AUDPS* measured at the beginning and after five passages of experimental evolution for viruses evolved in standard (upper) and in drought conditions (lower) for each one of the *A. thaliana* accessions (columns). Significance values from pairwise *post hoc* Bonferroni tests in the GLM described in Eq. 1; in all cases $P \leq 0.004$. (C) Mutations found in the standard- (left) and drought-evolved (right) lineages. Each square corresponds with a protein indicated in the lowest row

(proportional to the cistron size). Nonsynonymous mutations are indicated with the new amino acid in red.

As an intrinsically disordered viral protein[20], VPg plays a role in virus-virus and virus-host protein-protein interaction networks[21,22]. Therefore, VPg is involved in multiple processes such as virus movement, viral RNA replication and suppression of host RNA silencing[23,24]. The functional effects of the mutations in the VPg protein were studied *in silico* using SNAP2 webserver, which provides a function-effect score for all possible variants at each residue of the protein[25]. Mutations fixed in standard-evolved viruses were predicted to have a significantly weaker effect (mean ±1 SD = –0.400 ±22.831) than the ones fixed in drought-evolved viruses (22.067 ±26.797) (two-samples *t*-test, $t_{28} = 6.109$, $P = 0.020$), which are predicted to be more structurally and functionally disruptive. We hypothesize that under abiotic stress circumstances, more disruptive changes in VPg were selected in order to respond to the perturbations in the host gene expression.

Changes in host's transcriptomes when facing drought and virus infection. The whole-genome transcriptomic profiles of plants grown in drought conditions and infected with the drought-evolved viruses were compared with the transcriptomes of plants kept in standard conditions and infected with the standard-evolved viruses (Fig. 2). The number of differentially expressed genes (DEGs) was low in the accessions of G1. *Ler*-0 had five over- and four under-expressed genes while St-0 had eight over- and 21 under-expressed ones (Fig. 2A). In contrast, in the accessions belonging to G2, the number of DEGs was higher in both Oy-0 (2575 over- and 2656 under-expressed) and in Wt-1 (408 over- and 259 under-expressed) (Fig. 2A).

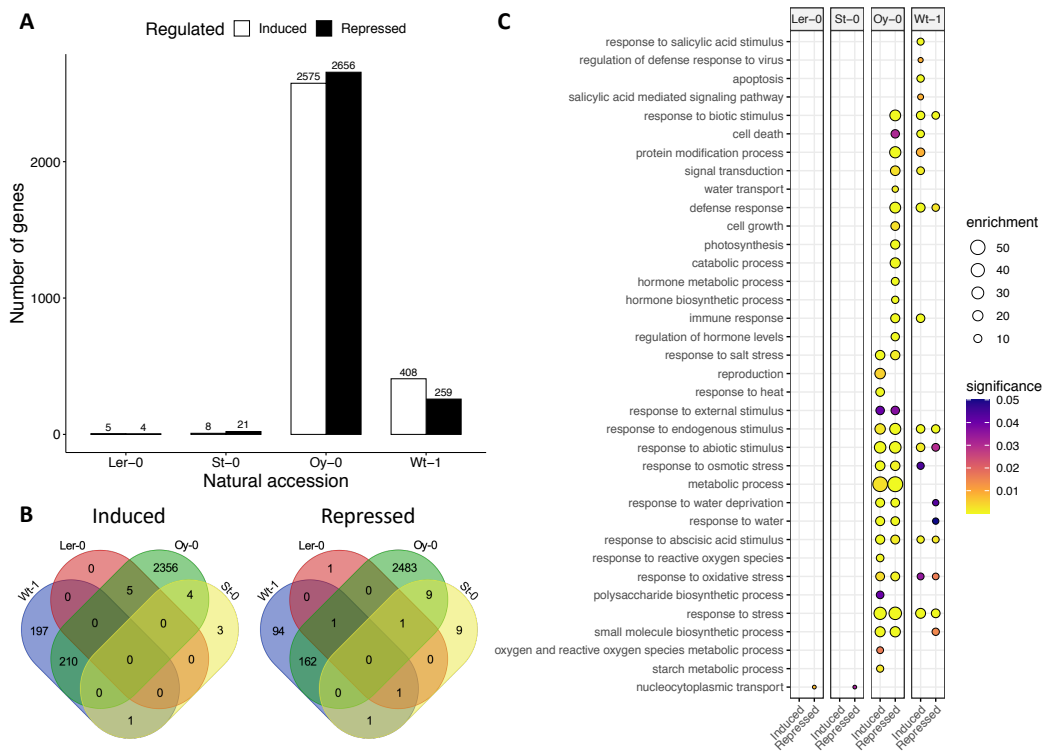

Fig. 2. Transcriptomic responses of different *A. thaliana* accessions to TuMV infection. In each accession, the response of a pool of eight to ten plants infected with each one of the corresponding drought-evolved TuMV lineages was compared to the response of plants infected with the standard-evolved viral lineages. (A) Number of DEGs obtained for each accession. Over-expressed genes are represented by white bars and under-expressed genes by black bars. (B) Over- (left) or under-expressed (right) DEGs shared between different accessions. (C) Gene ontology analysis for DEGs between drought-evolved viruses and standard-evolved ones for each one of the accessions (columns). Circle size represents the level of enrichment and color indicate adjusted *P* values.

All accessions share a few over- or under-expressed genes with other accessions (Fig. 2B). L*er*-0, Oy-0 and St-0 show in common the under-expression of *PSEUDO-*

142 *RESPONSE REGULATOR 5* (*PRR5*), a gene associated with circadian biological
143 events. The PRR5 protein is a transcriptional repressor of the MYB-related
144 transcription factors involved in circadian rhythm *CIRCADIAN CLOCK*
145 *ASSOCIATED 1* (*CCA1*) and *LATE ELONGATED HYPOCOTYL 1* (*LHY1*). The
146 repression of *PRR5* would lead to higher levels of *LHY1* expression, a gene that
147 promotes expression of ABA-responsive genes responsible for increased tolerance
148 to drought[27]. *FLAVIN-BINDING KELCH REPEAT F BOX 1* (*KFK1*), another gene
149 involved in circadian rhythm, is also under-expressed in multiple accessions (L*er*-0,
150 St-0 and Wt-1). The protein FKF1 stabilizes *CONSTANS* (*CO*) expression.
151 Therefore, a reduction in *FKF1* expression will result in lower *CO* activity. A *CO*-
152 like gene in rice has been shown to reduce drought resistance when overexpressed
153 and to increase drought tolerance when knocked out[28]. So, all accessions share genes
154 involved in the regulation of circadian rhythm. Furthermore, the functional profiling
155 of the DEGs (Supplementary File S1) show a significant over-representation of genes
156 involved in circadian rhythm in the under-expressed DEGs of the G1 accessions.
157 This observation goes in line with recent evidence supporting circadian clock as a
158 contributor to plants tolerance and acclimation to abiotic stresses[29]. Circadian
159 rhythms also seem to play an important role in infection, as it affects traits that could
160 provide an advantage to parasites, hosts, both or neither[30]. In Oy-0 plants, *WRKY*
161 *DNA-BINDING PROTEIN 57* (*WRLY57*) is over-expressed. This gene encodes for
162 the protein WRKY57, that confers drought tolerance in *A. thaliana*[31]. In this
163 accession there is also an overexpression of the *THREALOSE-6-PHOSPHATE*
164 *PHOSPHATASE F* (*TPPF*) gene, whose overexpression increases drought tolerance
165 in *A. thaliana* through accumulation of soluble sugars[32].

Focusing in biological functions, G1 accessions have no significant functional enrichment among DEGs, but for both accessions there is a reduction in DEGs involved in the nucleocytoplasmic transport. It has been described that the disruption of genes involved in nuclear transport leads to the increase in drought tolerance[33]. In the case of G2 accessions, the number of enriched and depleted biological categories were higher than in the accessions of G1. However, there were no obvious similarities in the pattern of enrichment between the two accessions of the G2. In Wt-1 there is an enrichment of the defense response to virus infection, which may explain why under drought conditions the virus had more difficulties to adapt and two lineages were extinctic at early passages of the evolution experiment.

To further evaluate how each accession responded to virus infection and drought, the expression of a set of key genes in stress regulation (Fig. 3) were quantified in the combination of all environmental and virus evolution conditions. Comparison of the gene expression in plants infected with standard- and drought-evolved viruses showed that most of the differential expression happens in the drought environment. Even in these stressful conditions, the number of genes differentially expressed depends on the plant accession that the viruses were evolved in.

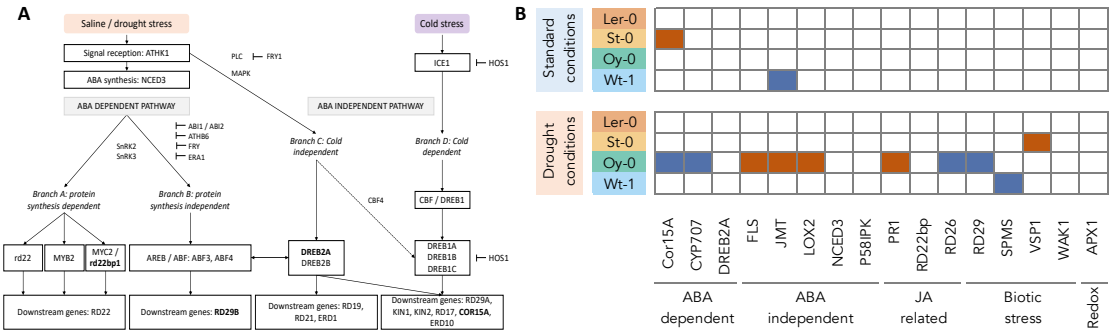

Fig. 3. (A) Schematic representation of *A. thaliana* network regulating the response to drought stress; in bold some of the genes whose expression was evaluated. (B)

Comparation of the $2^{-\Delta\Delta C_T}$ values of plants infected with standard- or drought-evolved viruses. Significant differences are marked in blue when the levels are significantly higher in plants infected with standard-evolved viruses and in orange when infected by drought-evolved viruses (pairwise *post hoc* Bonferroni tests in the GLM model described in Eq. 2; in all cases $P \leq 0.040$). The accessions and the conditions where the sample was taken from are indicated in the left. Participation of the measured genes in particular responses to stress are indicated under the table.

Our data suggests that virus adaptation under drought conditions results in a differential transcriptome change in their local hosts. Previous work has shown how the degree of adaptation of a potyvirus differentially affects the transcriptome of infected plants[34]. It also likely that drought- and standard-adapted viruses alter gene expression by manipulation certain methylation patterns in their host, as recently observed in TuMV lineages *naïve* and well adapted to *A. thaliana*[35], though we have not tested this hypothesis here.

Changes in host-virus interactions. Virus infection can alter the tolerance of plants to drought. We studied the survival of each accession to drought conditions when not infected or when infected with standard- or drought-evolved viruses (Fig. 4A). L*er*-0 showed almost no survival regardless of their infection status, with no significant differences in mean probability of survival between non-infected plants and plants infected with the standard-evolved viruses (mean difference ±1 SD: 0.000 ±0.128, $P = 1.000$) or plants infected with the drought-evolved viral lineages (0.029 ±0.128, $P = 1.000$). For the rest of the accessions, plants infected with the standard-evolved viruses had a higher mean survival probability to drought than non-infected

plants, thought the differences were not statistically significant (Fig. 4A; St-0: 0.308 ±0.128, $P = 0.490$; Oy-0: 0.356 ±0.128, $P = 0.202$; Wt-1: 0.352 ±0.128, $P = 0.203$). In sharp contrast, the comparison of mean drought survival probabilities of plants infected with drought-evolved viruses, showed that drought tolerance was significantly higher than in non-infected plants (Fig. 4A; St-0: 0.444 ±0.128, $P = 0.023$; Oy-0: 0.606 ±0.128, $P < 0.001$; Wt-1: 0.592 ±0.157, $P = 0.007$). It has been observed that in situations of abiotic stress viruses can promote host survival and therefore their own survival[36]. We observed that the promotion of host survival to a given abiotic stress is higher when the virus was evolved in plants submitted to such constant stress. In other words, viruses can adapt to promote host tolerance to the environmental perturbations. This may lead to a transition into a mutualistic relationship between the virus and the host as both of them benefit from the infection: the virus is able to replicate and spread while the infected host acquires a physiological and/or morphological change that promotes its survival in the adverse environment.

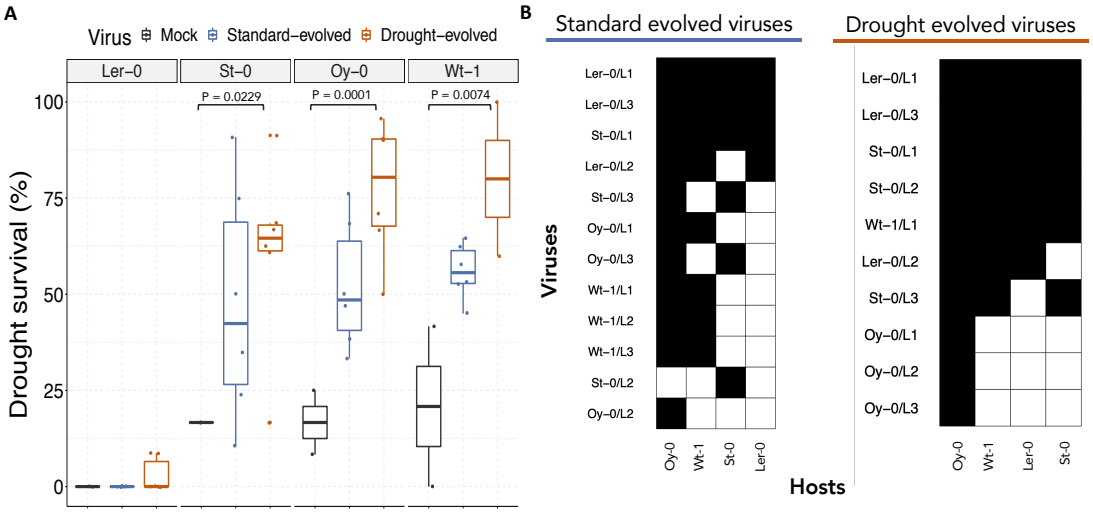

Fig. 4. Host-virus interactions. (A) Host survival in severe drought stress in different accessions. Comparison between non-inoculated plants (gray), plants inoculated with the standard- (blue) and with the drought-evolved (orange) viruses. Significant differences are marked with brackets and the *P* values are indicated (pairwise *post hoc* Bonferroni tests in the GLM described in Eq. 3). (B) Packed infection matrices in standard conditions for standard- and drought-evolved viruses. Viruses used as inocula are ordered (from the most generalist to the most specialists) in the rows and the different hosts (from the most permissive to the less one) in the columns. Black squares represent virus-host combinations in which *AUDPS* was equal or greater than the value observed for the corresponding viral lineage in its corresponding local host.

218

219 To analyze the specificity of adaptation of each evolved TuMV lineage, we
220 inoculated the 22 evolved viruses into each one of the four accessions and their
221 performance was evaluated using *AUDPS*. With this data, we built up two infection
222 matrices (Fig. 4B), one for plants inoculated with standard-evolved and another with
223 drought-evolved viruses. In each matrix, black squares represent host-virus
224 combinations in which *AUDPS* was equal or greater than the value observed for the
225 viral lineage in its corresponding local host. Therefore, the upper rows correspond
226 to more generalist lineages while the lower ones correspond to more specialist ones.
227 In general, viruses evolved in accessions from G1 (L*er*-0 and St-0) are more
228 generalist than viruses evolved in accessions from G2 (Oy-0 and Wt-1 lineages).
229 Likewise, plants from G2 are more susceptible to infection than those from G1. This
230 indicates that accessions which are more permissive to infection gave rise to less
231 pathogenic viruses, while the more restrictive accessions selected for viruses with

232 greater pathogenicity. Similar results have been previously reported for potyvirus -
233 *A. thaliana* pathosystems[37,38].

234 To quantify the degree of specialization in the infection matrices, we calculated
235 the partner diversity *d*' index[39]. For the infection matrix estimated for standard-
236 evolved viruses the value is 372-fold higher (*d*' = 0.037) than in the matrix estimated
237 for drought-evolved viruses (*d*' = 0.0001). This indicates that virus specialization
238 evolved when the host plants were facing more permissive standard growth
239 conditions.

240 Finally, we evaluated the nestedness and modularity of the two matrices. The
241 infection matrix estimated for the standard-evolved viruses shows a significant *T*-
242 nestedness[40] (Fig. 4B, left; $T = 30.441$, $P = 0.029$), while the matrix estimated for the
243 drought-evolved viruses did not show significant nestedness (Fig. 4B, right; $T =$
244 18.506, $P = 0.053$). This suggests that virus evolution in standard conditions selects
245 for a gene-for-gene kind of interaction mechanism in which more susceptible hosts
246 select for more specialized viruses while more resistant viruses select for more
247 generalist viruses. However, under drought conditions this highly specific
248 mechanism has been overcame. We also studied the modularity of the infection
249 matrices, as the presence of modules suggest that common selective constraints are
250 imposed by different hosts and similar evolutionary solutions are found by viruses.
251 Both matrices show significant *Q*-modularity[41] ($P = 0.019$ for standard-evolved
252 viruses and $P < 0.001$ for the drought-evolved ones), with the modularity observed
253 in the matrix of the standard-evolved viruses being 1.735 times larger than in the
254 matrix of the drought-evolved ones.

255 Next, we inoculated all of the viral lineages in their corresponding local
256 accessions in both standard and drought conditions. We found no changes in the

257 viral load of both viruses in all accessions (Fig. 5A). Despite not being able to
258 observe significant differences in the virus accumulation, viruses evolved in Wt-1
259 have a lower viral load that results in a significant reduction of *AUDPS* (Fig. 5B).
260 The drought-evolved viruses performed worse in Wt-1 accessions than the standard-
261 evolved viruses, an observation that contributes to better understand why two
262 lineages of Wt-1 drought-evolved viruses could not adapt and ended up going extinct
263 at early passages of the evolution experiment. Previously, Aguilar et al. observed
264 that potato virus X and plum pox virus conferred drought-tolerance in *N.*
265 *benthamiana* and *A. thaliana*[42]. This tolerance was enhanced when a virulence
266 protein was over-expressed during the virus infection. In contrast, our results suggest
267 that the enhanced host drought tolerance triggered by drought-evolved viruses does
268 not occur due to a higher virulence.
269

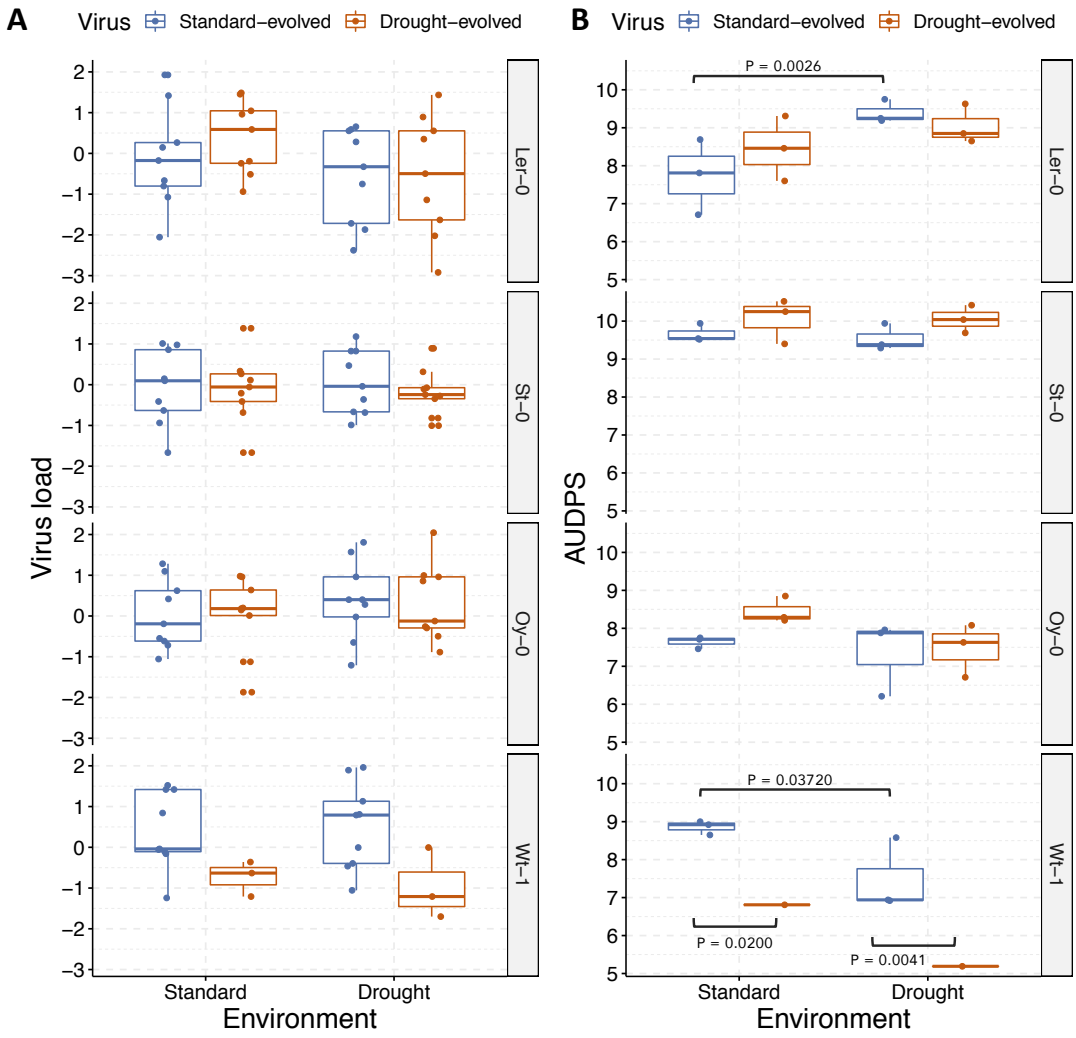

Fig. 5. Two fitness-related traits quantified in standard and drought conditions; blue color for standard- and orange for drought-evolved viruses. Significant differences are marked with brackets and the *P* values are indicated (pairwise *post hoc* Bonferroni tests in the GLM described in Eq. 2). (A) *Z*-scores of viral loads quantified as copies of *CP* RNA per ng of total RNA (the presence of this protein ensures that the whole virus genome was transcribed and no defective particles were quantified). (B) Infection progression measured as *AUDPS*.

Differences in hormones profiles. Plant response to biotic and abiotic stresses depends on the fine tuning among different phytohormones. We have studied the hormonal levels of plants in both environmental conditions, paying attention to

differences among non-inoculated plants and plants infected with the drought- and standard-evolved viruses (Fig. 6). In both standard and drought conditions the levels of salicylic acid (SA) were significantly higher in infected plants (regardless in which conditions the virus was evolved) than in non-infected plants. This increase is expected as SA is a key component in defense signaling, inducing the expression of many defense-related genes[43]. However, SA not only plays a role in plant defense but also in plant growth regulation and responses to abiotic stresses[44]. Xu et al. found high SA concentrations in plants infected with brome mosaic virus (BMV) and cucumber mosaic virus (CMV) although it could not be unambiguously associated with the improved drought tolerance provided by the infection[12]. Aguilar et al. using SA-deficient transgenic lines observed that SA has a role in the tolerance provided by the virus infection[42]. We have observed an increase in SA levels when plants were infected with either standard- or drought-evolved viruses in all accessions. But we have not found significant difference between SA levels in plants infected with viruses evolved in standard or drought conditions. Therefore, the enhanced tolerance caused by drought-evolved viruses cannot be explained by the SA levels, suggesting that other plant hormones could be implicated in the enhanced tolerance provided by drought viruses. In consequence, abscisic acid (ABA), polyamines (PA), jasmonic acid (JA), jasmonoyl isoleucine (JA-Ile), oxo-phytodienoic acid (OPDA), and indole-3 acetic acid (IAA; the main auxin) levels were also quantified. In standard growth conditions, the only significant difference in the hormonal levels between plants infected with standard- and drought-evolved viruses was observed for the L*er*-0 accession, where the level of PA is significantly higher in plants infected with standard evolved-viruses (Fig. 6A). In drought conditions, the differences are significant for viruses evolved in Oy-0, with plants infected with the standard-

299 evolved viruses had higher levels of ABA and OPDA than drought evolved ones

300 (Fig. 6A).

301

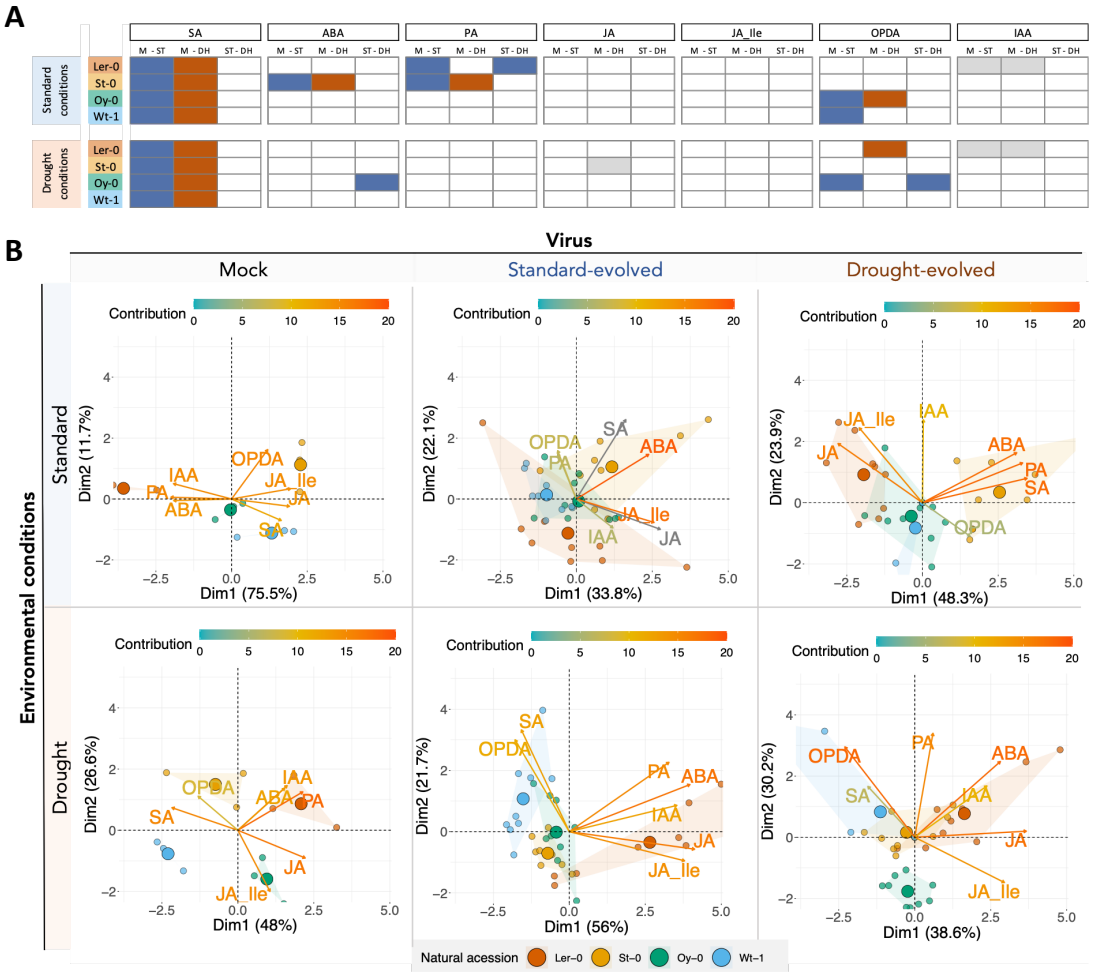

Fig. 6. Quantification of stress-related hormones. (A) Comparison of the hormone profiles between non-infected plants (M), plants infected with standard- and drought-evolved viruses. Significant (pairwise *post hoc* Bonferroni tests the GLM described by Eq. 2; in all cases $P \leq 0.039$) differences in the comparation are marked in color: blue when the levels are significantly higher in samples from plants infected with standard-evolved viruses, orange for plants infected with drought-evolved viruses and grey for non-infected plants. The accessions and the conditions where the sample was taken are indicated in the left. (B)

Principal component analysis of the quantified hormones. In all cases, the first two components explain more than 55% of observed variability.

302

303 A principal component analysis (Fig. 6B) shows that the hormonal profile of the
304 four accessions differs depending on the infection status and the environmental
305 condition in which the plants grew. The grouping of the samples in accessions is
306 clear when plants are non-infected or in drought conditions, the response being more
307 homogeneous during infections in standard-conditions. Interestingly, ABA shows
308 an expression profile in non-infected plants grown in standard conditions (over the
309 *x*-axis of the second quadrant) that markedly differs from the patter shown in non-
310 infected plants grown in drought conditions, which actually is similar to the pattern
311 shown by all infected plants, regardless the virus type (in all cases lying in the first
312 quadrant). SA clearly distinguishes between infected plants grown in standard (first
313 quadrant) and drought conditions (second quadrant) (Fig. 6B). JA and JA-Ile also
314 show an interesting pattern, highly correlated: while the vectors lie close to the *x*-axis
315 of the first quadrant in non-infected plants grown in standard conditions, they both
316 move to the second quadrant in plants infected with drought-evolved viruses kept in
317 standard conditions and move to the fourth quadrant in all other situations.
318 In summary, we have observed that TuMV lineages evolved in drought
319 conditions enhanced *A. thaliana* tolerance to drought. It was observed before that a
320 virus can confer drought tolerance to their host but, to our knowledge, this is the first
321 time it was explored how abiotic stresses shape the evolution of a host-virus
322 interaction. In our study we have observed that the response to virus infection in
323 drought conditions is diverse within the same species, suggesting that the
324 mechanisms used by viruses to induce drought tolerance are not universal and

different mechanisms could be activated depending on the virus and the host genotypes. Xu et al. observed that drought tolerance improved with virus infection and found an increase in several osmoprotectants and antioxidants and that changes in the metabolite profiles were different depending on the pathosystem[12]. As an example: trehalose, putrescine and SA levels were increased in virus-infected plants under water deficit conditions but proline, ascorbic acid and sucrose were increased only in BMV-infected rice while galactose, maltose and anthocyanins were only increased in CMV-infected beet. Aguilar et al. found that hormone levels and metabolite profiles also vary among plants under drought-conditions depending on the virus infecting them[42]. Gorovits et al. found that tomato plants infected with tomato yellow leaf curl virus had tolerance to several abiotic stresses[45]. This tolerance was found to be achieved by the viral repression of the ubiquitin 26S proteasome degradation and heat shock transcription factors. The variety in the mechanisms found in different pathosystems matches the diversity we found within *A. thaliana* accessions.

Bergès et al. illustrated a high level of variability in the response to virus infection and drought within the same species[46]. They studied the response of multiple *A. thaliana* accessions to cauliflower mosaic virus (CaMV) infection in drought conditions. They found that under water-stress symptom appearance and rate of systemic spread was not changed in some accessions while in others it was altered, increasing in some accessions and decreasing in others. CaMV causes death in some of the *A. thaliana* accessions they selected. Interestingly they found that most of the studied accessions had a bigger survival rate during infection when they were cultivated in drought conditions compared to well-watered conditions. The beneficial virus-host interaction under drought conditions may also expand into other

organisms that interact with the pathosystem, such as viral vectors. For example, in the pathosystem wheat - barley yellow dwarf virus it was shown that drought and virus infection enhance the performance of the aphid vector *Rhopalosiphum padi*[47].

So, it has been observed that drought conditions may cause a virus to promote stress tolerance to the host and a higher tolerance to the virus infection. These observations show how drought conditions shape the virus-host interaction into a less pathogenic outcome, with viruses evolved in drought conditions proving more beneficial to their hosts.

Conclusions

The environment where a virus evolves influences progression of the viral infection. In general, plant viruses can adapt to extreme drought conditions but in certain host accessions this process can be more difficult. In this type of hosts, viral populations might be driving to extinction or will reach a lower fitness than they would in standard conditions. In our experimental evolution this fitness decline has been observed in the two lineages evolved in Wt-1 that were extinct. Nevertheless, in other host accessions plant viruses adapted and increased their fitness equally well regardless of the watering conditions. The environment also influences the mechanisms of selection in virus evolution: the evolutionary solution reached by viruses evolved in standard conditions matched a gene-for-gene kind of interaction mechanism while viruses evolved under stressful drought conditions did not. Implying that a gene-for-gene interaction mechanism likely requires a precise fine-tuning, which can be achieved under the soft selection regime imposed by the standard conditions, while it cannot be reached in the strong selection regime

374 imposed by the physiological changes suffered by plants grown under strong drought
375 conditions.

376 During their evolution in drought conditions, viruses were selected to confer a
377 higher drought tolerance to the hosts they were infecting. Therefore, under
378 conditions of drought stress, infected plants will have an enhanced tolerance to water
379 deficit in their environment. This interaction will promote the plant host survival and
380 hence virus replication and transmission will be increased. The underlaying
381 mechanism that promotes drought tolerance seems to be specific for each accession.
382 Hosts whose response to infection was similar also had similar responses to drought
383 during the infection but, even within groups, each accession had a particular
384 response. This difference in the host response is probably triggered by adaptations
385 in the viral VPg protein. This highly multifunctional protein accumulated mutations
386 in all lineages, but mutations found in drought-evolved lineages were predicted to be
387 more functionally disruptive than the ones fixed in lineages evolved in standard
388 conditions.

389 The fact that viruses evolved in drought promoted a higher rate of plant survival
390 demonstrates how virus-host interactions are dependent on the environment and their
391 natural history. Here we have showed that under environmental perturbations, virus-
392 host interactions can evolve from pathogenic to mutualistic in a relatively short
393 evolutionary time.

394

395

396 **Methods**

397 **Plant material.** Four accessions of the model plant *A. thaliana* were used as hosts.
398 These accessions showed different response to potyvirus infection[17], being classified

399 into two groups based on their response to the viral infection: (*i*) G1, inducing a
400 severe infection and tending to up-regulate defense genes and to shut down the
401 production of cell wall components (St-0 and L*er*-0) and (*ii*) G2, with milder
402 symptoms and lower virus accumulation, tending to up-regulate genes involved in
403 abiotic stress and cell wall construction (Wt-1 and Oy-0).

404 The selected accessions were exposed to standard watering and drought
405 conditions. Standard conditions consisted of watering every two days until the plants
406 were harvested at 14 days post inoculation (dpi). Drought conditions consisted of
407 water withdrawal from 7 dpi until 14 dpi (time at which the plant tissue was
408 harvested).

409 The evolution experiment was performed in a BSL-2 greenhouse at 24 °C with
410 16 h light:8 h dark photoperiod. The rest of the experiments were done in a growing
411 chamber at 24 °C with 16 h light:8 h dark photoperiod, 45% relative humidity and
412 125 μmol $m^{-2}s^{-1}$ of light intensity (1:3 mixture of 450 nm blue and 670 nm purple
413 LEDs).

414

415 **Experimental virus evolution.** The infections were initiated using homogenized
416 TuMV-infected tissue preserved at −80 °C. This virus stock was created from
417 infected tissue of *N. benthamiana* plants previously inoculated with an infectious
418 clone derived from TuMV isolate YC5 (GenBank accession AF530055.2) from calla
419 lilly (*Zantedeschia* sp.)[48].

420 The stock was used to inoculate four *A. thaliana* accessions. The inoculum used
421 consisted of 100 mg of homogeneous N_2-frozen infected tissue mixed with 1 mL of
422 phosphate buffer and 10% Carborundum (100 mg/mL). For each accession 10 plants
423 were inoculated and kept in standard conditions (well-watered) until infected plants

were harvested at 14 dpi and another 10 under drought conditions (no watering from 7 dpi until the harvest at 14 dpi). Only the symptomatic infected plants were collected, making a pool of infected tissue from each condition and accession, using it as inoculum to start a five-passage evolution. For each accession and condition, three lineages were established (Fig. 1A).

Area under the disease progression stairs curve (*AUDPS*). Upon inoculation, plants were inspected daily for visual symptoms. The data of infectivity during the 14 dpi was used to calculate the *AUDPS* as described in ref. 18. This formula transforms data from disease progression, allowing us to express the virulence and dynamics of the disease into a single figure. The *AUDPS* ranges between zero and the total number of observation time points along the experiment; larger *AUDPS* values mean that the virus infects a higher number of plants more quickly. *AUDPS* values were computed using the agricolae R package version 1.3-2 with R version 3.6.1 in RStudio version 1.2.1335.

Depending on the particular experiment being analyzed, *AUDPS* data were fitted to two fully factorial generalized linear model (GLM). In the first type of experiments, plant accession (*A*) and environmental conditions (*C*) were treated as orthogonal factors and evolutionary passage (*t*) as a covariable. The full model equation reads

$$AUDPS_{ijk}(t) \sim \alpha + A_i + C_j + P + (A \times C)_{ij} + (A \times t)_i + (C \times t)_j + (A \times C \times t)_{ij} + \varepsilon_{ijk}, \quad \text{(Eq. 1)}$$

where α stands for the intercept, and ε_{ijk} represents the Gaussian error associated with each individual *k* plant measured at passage *t*.

In the second type of experiments, plant accession (*A*), environmental conditions being tested (*C*), and environmental conditions where the virus evolved (*E*) were treated as orthogonal factors. The full model equation now reads

$$AUDPS_{ijkl} \sim \alpha + A_i + C_j + E_k + (A \times C)_{ij} + (A \times E)_{ik} + (C \times E)_{jk} + (A \times C \times E)_{ijk} + \varepsilon_{ijkl}, \quad \text{(Eq. 2)}$$

where α and ε_{ijkl} had the same meaning than in the Eq. 1. In both cases, a Gaussian distribution and identity link function were chosen based on the minimal *BIC* value among competing models. Hereafter, all GLM fitting were done with SPSS version 26 software (IBM, Armonk, NY).

***In silico* evaluation of functional effects associated with observed mutations in VPg.** The functional effects of the mutations in the VPg protein were studied *in silico* using the Screening for Nonacceptable Polymorphisms (SNAP2) web server (rostlab.org/services/snap2web/; last accessed May 20, 2020). SNAP2 machine learning tools provide a score for all possible variants at each residue of the protein[25]. This score indicates if there is any effect of the variant in the protein function, regardless if the effect is positive or negative. The score value ranges between −100 (no effect) and 100 (maximal effect).

Next generation sequencing. RNA was extracted from infected plant tissue using Plant RNA Isolation Mini Kit (Agilent). The quality of the RNAs used to prepare RNA-seq libraries was checked with the Qubit RNA BR Assay Kit (ThermoFisher). SMAT libraries, Illumina sequencing (paired end, 150 bp), and quality-check of the mRNA-seq libraries were done by Novogene Europe (UK). Seventeen bases from the 5' end and twelve from the 3'of the reads were trimmed with cutadapt using

473 cutadapt[49] v2.10. Trimmed sequences were mapped with HiSat2[50] v2.1.0 to the
474 ENSEMBL release 47 of the *Arabidopsis* TAIR10 genome assembly. For viral
475 genome SNP calling, trimmed reads were mapped with HiSat2 to the TuMV isolate
476 YC5 (GenBank, AF530055.2) with a modified minimum score parameter (*L*, 0.0,
477 −0.8) to allow more mismatches. Resulting SAM files were BAM-converted, sorted,
478 indexed and analyzed with SAMtools[51] v1.10. SNP calling was performed using
479 bcftools v1.6 by first using the mpileup subroutine. Read counting in features was
480 done with htseq-count, using The *Arabidopsis* Reference Transcript Dataset
481 (AtRTD2)[52] as input annotation file. Differential expression analysis was done with
482 DESeq2[53] v1.24.0, considering only genes having a total of at least 10 reads for each
483 pairwise comparison. Characterization of DEGs was done with plant GOSilm
484 implemented in the Cytoscape plugin Bingo[54] and MapMan[55]. Functional profiling
485 was done using gProfiler[56].
486
487 **RNA isolation and cDNA synthesis.** Total RNA was extracted from plant tissues
488 using Total Quick RNA Cells and Tissues Kit (Talent SRL), following the protocol
489 established by the manufacturer. Further, DNase treatment (TURBO DNA-free Kit,
490 Ambion) was performed to remove genomic DNA. RNA quantification was
491 performed by spectrophotometric analysis and its integrity was checked by
492 denaturating agarose gel electrophoresis. The absence of genomic DNA from the
493 RNA samples was additionally tested by the null PCR amplification of the universal
494 rDNA primer pair ITS1/ITS4. Then cDNA was synthetized from 2 µg of total RNA,
495 using SuperScript III H-Reverse Transcriptase (Invitrogen) and 100 pmol of random
496 hexamers (Pharmacia Biotech) according to suppliers' instructions.
497

Quantitative RT-PCR analysis. Quantitative real time PCR (RT-qPCR) was performed on a Thermal Cycler CFX96™ Real-Time System (BIO-RAD) using Power SYBR® Green PCR Master Mix (Applied Biosystems), 11 µL reactions contained 4.9 µL of 1:6 diluted cDNA samples (8.5 ng of cDNA), 0.3 µL (300 nM) of each primer (forward and reverse) and 5.5 µL of SYBR® Green PCR Master Mix. PCR conditions were as follows: two initial steps of 50 °C for 2 min and 95 °C for 2 min, followed by 40 cycles of 95 °C for 30 s and 60 °C for 30 s. Afterwards, the dissociation protocol was performed to identify possible unspecific products. Three biological replicates per treatment were analyzed by RT-qPCR. For each transcript, the threshold cycle (C_T) was determined using Bio-Rad CFX Manager 3.1 software. Primers used in the RT-qPCRs are described in Supplementary file S2.

Viral load was estimated by RT-qPCR using primers that amplify the *CP*. Viral load data, that were fitted to a fully factorial GLM with the same factors and structure than Eq. 2.

Infection matrices. A full cross-infection experiment was performed where all the 22 evolved lineages were inoculated into ten plants of all four accessions. Infection matrices were analyzed using tools borrowed from the field of community ecology[57]. The statistical properties of the resulting infection matrices were evaluated using the bipartite R package version 2.11[58] in R version 3.6.1 (R Core Team 2016) in RStudio version 1.2.1335. Three different summary statistics were evaluated: *T*-nestedness[40], *Q*-modularity[41], and overall specialization *d*' index[39]. *d*' is based in Kullback–Leibler relative entropy, that measures variation within networks and quantifies the degree of specialization of elements within the interaction network. Statistical

522 significance of nestedness and modularity was evaluated using Bascompte et al. null
523 model[40].
524
525 **Survival analysis.** Lineages evolved under drought or standard conditions in a
526 certain accession where inoculated in 24 plants of the same accession. Twenty-four
527 plants were mock-inoculated as control. Seven dpi, a severe drought was simulated
528 in the plants by withdrawing water for 14 days. After this period of drought plants
529 were watered again during seven days and their survival was evaluated. This
530 experiment was done twice for each one of the four accessions.
531 Survival frequency (*S*) data were fitted to a factorial GLM in which natural
532 accession (*A*) and type of virus inoculum (*V*) were treated as orthogonal random
533 factors. A Binomial distribution and logit link function were chosen based on the
534 minimal *BIC* value among competing models. The full model equation reads
535 $S_{ijk} \sim \Sigma + A_i + V_j + (A \times V)_{ij} + \varepsilon_{ijk}$, (Eq. 3)
536 where Σ corresponds to the model intercept, and ε_{ijk} represents the Gaussian error
537 associated with each individual *k* plant.
538
539 **Hormone quantification.** Hormone extraction and analysis were carried out as
540 described in ref. 59 with few modifications. Briefly, plant tissue was extracted in
541 ultrapure water in a ball mill (MillMix20, Domel, Železniki, Slovenija) after spiking
542 with 10 ng of [$^2H_2$]-IAA and 50 ng of the following compounds: [$^2H_6$]-ABA, [C_{13}]-
543 SA, [$^2H_3$]-PA and dihydrojasmonic acid. Following centrifugation, supernatants
544 were recovered and pH adjusted to 3.0. The water extract was partitioned against
545 diethyl ether and the organic layer recovered and evaporated under vacuum. The
546 residue was resuspended in a 10:90 CH_3OH:H_2O solution by gentle sonication. After

filtering, the resulting solution was directly injected into an ultra-performance LC system (Acquity SDS, Waters Corp., Milford, MA, USA). Chromatographic separations were carried out on a reversed-phase C18 column (Gravity, 50×2.1mm, 1.8-µm particle size, Macherey-Nagel GmbH, Germany) using a CH_3OH:H_2O (both supplemented with 0.1% acetic acid) gradient. Hormones were quantified with a TQS triple quadrupole mass spectrometer (Micromass, Manchester, UK). Multivariate analysis was perform using the package 'FactoMineR'[60] in R version 3.6.1 (R Core Team 2016) in RStudio version 1.2.1335.

Hormones concentration were fitted to a fully factorial GLM with the same factors and structure than Eq. 2.

References

1. Paez-Espino, D. et al. Uncovering Earth's virome. *Nature* **536**, 425–430 (2016).
2. Roossinck, M. J. The good viruses: viral mutualistic symbioses. *Nat. Rev. Microbiol*. **9**, 99–108 (2011).
3. Roossinck, M. J. 2012. Plant virus metagenomics: biodiversity and ecology. *Annu. Rev. Genet.* **46**, 359–369 (2012).
4. Roossinck, M. J. Plants, viruses and the environment: ecology and mutualism. *Virology* **479–480**, 271–277 (2015).
5. Roossinck, M. J. & Bazán, E. R. Symbiosis: Viruses as intimate partners. *Annu. Rev. Virol*. **4**, 123–139 (2017).
6. Prendeville, H. R., Ye, X., Morris, T. J. & Pilson, D. Virus infections in wild plant populations are both frequent and often unapparent. *Am. J. Bot*. **99**, 1033–1042 (2012).

571 7. González, R., Butković, A. & Elena, S. F. From foes to friends: Viral infections
572 expand the limits of host phenotypic plasticity. *Adv. Virus Res*. **106**, 85–121
573 (2020).
574 8. Shinozaki, K., Yamaguchi-Shinozaki, K. & Seki, M. Regulatory network of
575 gene expression in the drought and cold stress responses. *Curr. Opin. Plant Biol*.
576 **6**, 410–417 (2003).
577 9. Atkinson, N. J. & Urwin, P. E. The interaction of plant biotic and abiotic stresses:
578 from genes to the field. *J. Exp. Bot*. **63**, 3523–3543 (2012).
579 10. Atkinson, N. J., Lilley, C. J. & Urwin, P.E., Identification of genes involved in
580 the response of *Arabidopsis* to simultaneous biotic and abiotic stresses. *Plant*
581 *Physiol*. **162**, 2028–2041 (2013).
582 11. Dai, A. Increasing drought under global warming in observations and models.
583 *Nature Clim. Change* **3**, 52–58 (2013).
584 12. Xu, P. et al. Virus infection improves drought tolerance. *New Phytol*. **180**, 911–
585 921 (2008).
586 13. Prasch, C.M. & Sonnewald U. Simultaneous application of heat, drought, and
587 virus to *Arabidopsis* plants reveals significant shifts in signaling networks. *Plant*
588 *Physiol.* **162**, 1849-1866 (2013).
589 14. Dastogeer, K.M.G., Li, H., Sivasithamparam, K. & Jones, M.G.K. Fungal and
590 endophytes and a virus confer drought tolerance to *Nicotiana benthamiana*
591 plants thorugh modulating osmolytes, antioxidant enzymes and expression of
592 host drought responsive genes. *Environ. Exp. Bot*. **149**, 95-108 (2018).
593 15. Wolinska, J. & King, K. C. Environment can alter selection in host–parasite
594 interactions. *Trends Parasitol*. **25**, 236–244 (2009).

16. Lalić, J, Agudelo-Romero, P., Carrasco, P. & Elena, S. F. Adaptation of tobacco etch potyvirus to a susceptible ecotype of *Arabidopsis thaliana* capacitates it for systemic infection of resistant ecotypes. *Philos. Trans. R. Soc. B* **365**, 1997–2007 (2010).
17. Hillung, J., Cuevas, J. M. & Elena, S.F., Transcript profiling of different *Arabidopsis thaliana* ecotypes in response to tobacco etch potyvirus infection. *Front. Microbiol*. **3**, 229 (2012).
18. Simko, I. & Piepho, H. The area under the disease progress stairs: calculation, advantage, and application. *Phytopathology* **102**, 381-389 (2012).
19. Krasensky, J. & Jonak, C. Drought, salt, and temperature stress-induced metabolic rearrangements and regulatory networks. *J. Exp. Bot*. **63**, 1593–1608 (2012).
20. Hébrard, E. et al. Intrinsic disorder in viral proteins genome-linked: experimental and predictive analyses. *Virol. J.* **6**, 23 (2009).
21. Jiang, J. & Laliberté, J. F. The genome-linked protein VPg of plant viruses - a protein with many partners. *Curr. Opin. Virol*. **1**, 347–354 (2011).
22. Martínez, F. et al. Interaction network of tobacco etch potyvirus NIa protein with the host proteome during infection. *BMC Genomics* **17**, 87 (2016).
23. Revers, F. & García, J. A. Molecular biology of *Potyviruses*. *Adv. Virus Res*. **9**2, 101–199. (2015).
24. Cheng, X. & Wang, A. The *Potyvirus* silencing suppressor protein VPg mediates degradation of SGS3 via ubiquitination and autophagy pathways. *J. Virol*. **91**, e01478-16 (2017).
25. Hecht, M., Bromberg, Y. & Rost, B. Better prediction of functional effects for sequence variants. *BMC Genomics* **16**, S1 (2015).

620 26. Westwood, J. H. et al. A viral RNA silencing suppressor interferes with abscisic
621 acid-mediated signaling and induces drought tolerance in *Arabidopsis thaliana*:
622 Virus-induced drought tolerance. *Mol. Plant Pathol*. **14**, 158–170 (2013).
623 27. Adams, S. et al. Circadian control of abscisic acid biosynthesis and signaling
624 pathways revealed by genome-wide analysis of *LHY* binding targets. *New*
625 *Phytol*. **220**, 893–907 (2018).
626 28. Liu, J. et al. *Ghd2*, a *CONSTANS*-like gene, confers drought sensitivity through
627 regulation of senescence in rice. *J. Exp. Bot*. **67**, 5785–5798 (2016).1
628 29. Grundy, J., Stoker, C. & Carré, I. A. Circadian regulation of abiotic stress
629 tolerance in plants. *Front. Plant Sci*. **6**, 648 (2015).
630 30. Westwood, M.L. et al. The evolutionary ecology of circadian rhythms in
631 infection. *Nat. Ecol. Evol.* **3**, 552–560 (2019).
632 31. Jiang, Y., Liang, G. & Yu, D., Activated expression of *WRKY57* confers drought
633 tolerance in *Arabidopsis*. *Mol. Plant* **5**, 1375–1388 (2012).
634 32. Lin, Q. et al. Overexpression of the trehalose-6-phosphate phosphatase family
635 gene *AtTPPF* improves the drought tolerance of *Arabidopsis thaliana*. *BMC*
636 *Plant Biol*. **19**, 381 (2019).
637 33. Yang, Y., Wang, W., Chu, Z., Zhu, J.-K. & Zhang, H. Roles of nuclear pores
638 and nucleo-cytoplasmic trafficking in plant stress responses. *Front. Plant Sci*. **8**,
639 574 (2017).
640 34. Agudelo-Romero, P., Carbonell, P., Pérez-Amador, M. A. & Elena, S. F. 2008.
641 Virus adaptation by manipulation of host's gene expression. *PLoS ONE* **3**,
642 e2397.

643 35. Corrêa, R. L. et al. 2020. Viral fitness determines the magnitude of
644 transcriptomic and epigenomic reprograming of defense responses in plants.
645 *Mol. Biol. Evol*. **37**, 1866-1881 (2020).
646 36. Hily, J. M. et al. Environment and host genotype determine the outcome of a
647 plant-virus interaction: from antagonism to mutualism. *New Phytol*. **209**, 812–
648 822 (2016).
649 37. Hillung, J., Cuevas, J. M., Valverde, S. & Elena, S. F. Experimental evolution
650 of an emerging plant virus in host genotypes that differ in their susceptibility to
651 infection. *Evolution* **68**, 2467-2480 (2014).
652 38. González, R., Butković, A. & Elena, S. F. Role of host genetic diversity for
653 susceptibility-to-infection in the evolution of virulence of a plant virus. *Virus*
654 *Evol*. **5**, vez024 (2019).
655 39. Blüthgen, N., Menzel, F. & Blüthgen, N. Measuring specialization in species
656 interaction networks. *BMC Ecol*. **6**, 9 (2006).
657 40. Bascompte, J., Jordano, P., Melián, C. J. & Olesen, J. M. The nested assembly
658 of plant-animal mutualistic networks. *Proc. Natl. Acad. Sci. USA* **100**, 9389-
659 9387 (2003).
660 41. Newman, M. E. J. Modularity and community structure in networks. *Proc. Natl.*
661 *Acad. Sci. USA* **103**, 8577-8582 (2006).
662 42. Aguilar, E. et al. Virulence determines beneficial trade-offs in the response of
663 virus-infected plants to drought via induction of salicylic acid: trade-offs in
664 virus-infected plants to drought. *Plant Cell Environ*. **40**, 2909–2930 (2017).
665 43. Delaney, T. P. et al., A central role of salicylic acid in plant disease resistance.
666 *Science* **266**, 1247–1250 (1994).

667 44. Miura, K. & Tada, Y. Regulation of water, salinity, and cold stress responses by
668 salicylic acid. *Front. Plant Sci*. **5**, 4 (2014).
669 45. Gorovits, R., Sobol, I., Altaleb, M., Czosnek, H. & Anfoka, G. Taking advantage
670 of a pathogen: understanding how a virus alleviates plant stress response.
671 *Phytopathol. Res.* **1**, 20 (2019).
672 46. Bergès, S. E. et al. Natural variation of *Arabidopsis thaliana* responses to
673 cauliflower mosaic virus infection upon water deficit. *PLoS Pathog.* **16**,
674 e1008557 (2020).
675 47. Davis, T. S., Bosque-Pérez, N. A., Foote, N. E., Magney, T. & Eigenbrode, S.
676 D. Environmentally dependent host-pathogen and vector-pathogen interactions
677 in the barley yellow dwarf virus pathosystem. *J. Appl. Ecol*. **52**, 1392–1401
678 (2015).
679 48. Chen, C. C. et al. Identification of turnip mosaic virus isolates causing yellow
680 stripe and spot on calla lily. *Plant Dis*. **87**, 901-905 (2003).
681 49. Martin, M. Cutadapt removes adapter sequences from high-throughput
682 sequencing reads. *EMBnet j*. **17**, 10 (2011).
683 50. Kim, D., Paggi, J.M., Park, C., Bennett, C. & Salzberg, S.L. Graph-based
684 genome alignment and genotyping with HISAT2 and HISAT-genotype. *Nat.*
685 *Biotechnol.* **37**, 907–915 (2019).
686 51. Li, H. et al. The sequence alignment/map format and SAMtools. *Bioinformatics*
687 **25**, 2078–2079 (2009).
688 52. Zhang, R. et al. A high quality *Arabidopsis* transcriptome for accurate transcript-
689 level analysis of alternative splicing. *Nucleic Acids Res.* **45**, 5061–5073 (2017).
690 53. Love, M.I., Huber, W. & Anders, S. Moderated estimation of fold change and
691 dispersion for RNA-seq data with DESeq2. *Genome Biol.* **15**, 550 (2014).

692 54. Maere, S., Heymans, K. & Kuiper, M. BiNGO: a Cytoscape plugin to assess
693 overrepresentation of Gene Ontology categories in biological networks.
694 *Bioinformatics* **21**, 3448–3449 (2005).
695 55. Thimm, O. et al. mapman: a user-driven tool to display genomics data sets onto
696 diagrams of metabolic pathways and other biological processes. *Plant J.* **37**,
697 914–939 (2004).
698 56. Raudvere, U. et al. gProfiler: a web server for functional enrichment analysis
699 and conversions of gene lists (2019 update). *Nucleic Acids Res.* **47**, 191–198
700 (2019).
701 57. Weitz, J. S. et al. Phage-bacteria infection networks. *Trends Microbiol*. **21**, 82-
702 91 (2013).
703 58. Dormann, C. F., Gruber, B. & Fruend, J. Introducing the bipartite package:
704 analyzing ecological networks. *R News* **8**, 8-11 (2008).
705 59. Durgbanshi, A., et al. Simultaneous determination of multiple phytohormones
706 in plant extracts by liquid chromatography-electrospray tandem mass
707 spectrometry. *J. Agric. Food Chem*. **53**, 8437-8442 (2005).
708 60. Lê, S., Josse, J. & Husson, F. FactoMineR : An R Package for Multivariate
709 Analysis. *J. Stat. Soft.* **25**, 1–18 (2008).
710

711 **Acknowledgments**

712 We thank Francisca de la Iglesia and Paula Agudo for excellent technical assistance.
713 This work was supported by grants PID2019-103998GB-I00 and BES-2016-077078
714 (Agencia Estatal de Investigación - FEDER) to S.F.E. and R.G., respectively,
715 GRISOLIAP/2018/005 and PROMETEU2019/012 (Generalitat Valenciana) to S.F.E
716 and AICO/2019/150 (Generalitat Valenciana) to A.G.-C. Phytohormone

717 measurements were done at the Servei Central d'Instrumentació Científica (SCIC)
718 of the Universitat Jaume I.

719

720 **Author contributions**

721 R.G., A.B. and S.F.E. conceived and designed the study. R.G., A.B., J.M.L., I.M.,
722 and E.P.P. performed the evolution experiments, measured *AUDPS* and processed
723 the materials for RNA-seq. F.J.E. and P.C. quantified gene expression of marker
724 genes and evaluated viral loads. A.G.C. did hormone quantification. R.G. and A.B.
725 analyzed the RNA-seq data. R.G. and S.F.E. did all the statistical analyses. R.G.,
726 A.B. and S.F.E. wrote the manuscript. F.J.E., P.C., and A.G.C. contributed to
727 discussion of the results and writing of the manuscript.

728

729 **Competing interests**

730 The authors declare no competing interests.

Supplementary Materials

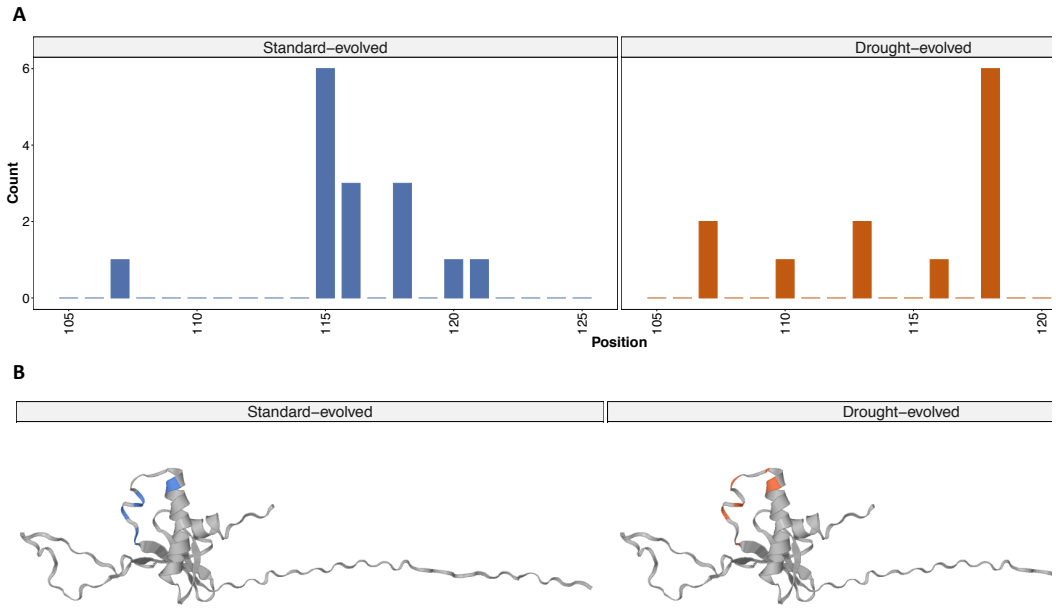

Supplementary Fig. S1. Nonsynonymous mutations in VPg for standard- (left, blue color) and drought-evolved (right, orange color) viruses. (A) Distribution of the mutations. (B) Location of the mutations in the predicted tridimensional structure of VPg.

Supplementary File S1. Functional profiling of the transcriptional response described in the section 'Changes in host's transcriptomes when facing drought and virus infection' (Excel).

Supplementary File S2. List of primers used in the gene expression quantifications (Excel).

Supplementary File S3. All raw data generated in this study (Excel).